P1.1 USING ANNULAR RINGS AND QUADRANTS TO CLIP POLYGONS REPRESENTING TROPICAL CYCLONE PRECIPITATION IN A GIS

Corene J. Matyas *
University of Florida, Gainesville, Florida

1. INTRODUCTION

A technique that researchers frequently employ to model the rainfall patterns of tropical cyclones (TCs) is dividing the storm into sections. Rao and Macarthur (1994) and Cerveny and Newman (2000) utilized a grid of squares and Rodgers et al. (1994a, 1994b) used a circular grid to explore the relationship between rainfall in the inner and outer regions of the storm and to characterize asymmetries present in the rainfall distributions across the storm track. This study imports radar reflectivity returns into a GIS, wherein a grid of annular rings and quadrants segments the rain shields of 13 U.S. landfalling TCs. The area covered by precipitation within each ring and quadrant is calculated for each radar composite in hourly intervals. Graphs resulting from the areal coverage data show how storm intensity, forward velocity, movement near mountainous terrain, interaction with middle latitude weather systems, and strong wind shear, affect the spatial distribution of rainfall within these TCs.

2. PROCEDURE

As this study requires data of high temporal and spatial resolution, base reflectivity radar returns are utilized to determine where rainfall occurred within each TC. These data are obtained from the Pennsylvania State University Department of Meteorology. Data are extracted for the scan nearest the top of each hour for each station within 400 km of the TC's circulation center. A Visual Basic script (NEX2SHP.exe) authored by Shipley (2000) georeferences each data file prior to its importation into ArcView GIS. To spatially analyze rainfall patterns over the entire TC's circulation, the radar scans from each station are merged into a single image. The conversion of these point data into polygon shapes occurs after the data are interpolated in 5 dBZ intervals using inverse distance weighting. The 20 dBZ contour line serves as the perimeter for the polygons (Matyas 2005) (Figure 1).

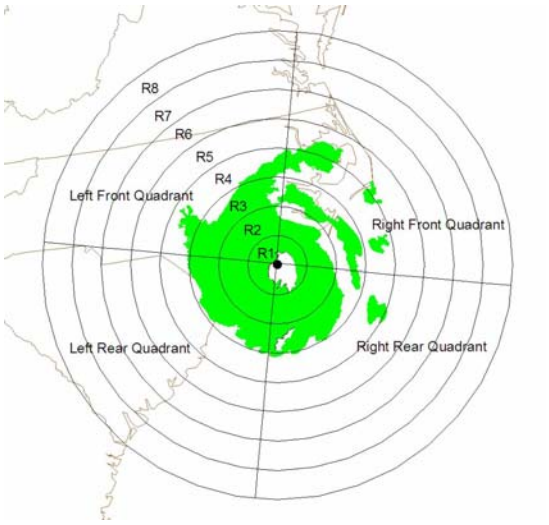

Figure 1. Polygons (green) representing the rain shield of Hurricane Bonnie (1998) and the circular grid used to clip these polygons. The green region contains reflectivity values above 20 dBZ.

Additional data pertaining to the storm's location, intensity, and synoptic history are required to complete the analysis. These data are obtained from the National Hurricane Center website (www.nhc.noaa.gov). As this study investigates rainfall pattern changes at hourly intervals, it is necessary to interpolate the six-hourly track and intensity data. The track data are also used to calculate storm speed and heading. Adding these data to the GIS allows the rainfall polygons for each storm to be associated with their position about the storm center.

* *Corresponding author address:* Corene J. Matyas, Univ. of Florida, Dept. of Geography, Gainesville, FL 32611-7315; e-mail matyas@ufl.edu

In the next phase of the analysis, the circular grid is created within the GIS (Figure 1). The storm's circulation center is buffered by eight circles spaced in 50-km increments. Four lines extend radially from the circulation center in 90° increments based on the storm's heading to create the quadrants. This circular grid is then used to clip the polygon shapes. The areas of all polygons within each grid section are then summed. The regions within each annular ring are labeled as shown in Figure 1. Because each ring covers a different-sized area, the summed polygon areas are divided by the total ring area to calculate the percentage of each ring that is occupied by the rain shield. The quadrant data are expressed as the area (in sq. km) of the rain shield contained within each quadrant. Adding the data from all four quadrants yields the total areal coverage of the rain shield.

A total of 468 hourly radar composites are processed in this manner. The number of composites analyzed for each TC varies (Table 1) because the entire rain shield must be within radar range before analysis can commence (Matyas 2005) and the earth's curvature limits the range of radar operation to approximately 235 km (Harasti et al. 2004). Graphs of these data are created for each TC to illustrate changes in the rain shield throughout the post-landfall period.

3. RESULTS

After a TC makes landfall, it is removed from its source of moisture and therefore, it is reasonable to assume that in the absence of other forcing mechanisms, the areal coverage of precipitation will diminish as the storm tracks inland. However, several physical forcing mechanisms affect the precipitation distribution of the thirteen TCs analyzed in this study. The following sections describe how storm intensity, forward velocity, movement near mountainous terrain, interaction with middle latitude weather systems, and strong wind shear cause rain shields to be come asymmetrically-distributed about the circulation centers of these 13 TCs during the post-landfall period. The effects of a specific forcing mechanism can be difficult to isolate as multiple forcing mechanisms often influence the precipitation distribution (Table 1).

Table 1. The number of observations analyzed for each tropical cyclone in the study. The following symbols denote a forcing mechanism experienced by a storm during its analysis period: * middle latitude effects, # mountainous terrain, ^ strong wind shear.

Tropical Cyclone	Year	No. of Obs.
Danny	1997	47
Bonnie	1998	16
Charley # ^	1998	48
Georges	1998	56
Hermine ^	1998	14
Bret #	1999	38
Dennis * # ^	1999	80
Harvey ^	1999	17
Irene	1999	14
Gordon * # ^	2000	63
Helene * ^	2000	38
Claudette #	2003	25
Isabel * #	2003	23

3.1 Storm Intensity

The results of this study show that TCs of hurricane intensity have more of their rain shield within R1 and R2 than do TCs of tropical storm or depression intensity. This finding agrees with that of both Rao and MacArthur (1994) and Cerveny and Newman (2000), who found a strong relationship between storm intensity and rainfall patterns. When faster tangential winds are present, more moisture evaporates from the ocean surface and can then circulate around the inner region of hurricanes (Rodgers et al. 1994b). Hurricane Georges, a category 2 storm on the Saffir-Simpson scale at landfall, (Figure 2) typifies this example, as rain shield coverage exceeds 80% in R1 and R2. As a TC weakens, precipitation no longer completely encircles the eye, causing a decrease in the values of R1 and R2. Georges moved slowly after landfall and remained near the coast, so it was not until approximately 24 hours post-landfall that precipitation decreased in the inner region of the storm (Figure 2).

3.2 Forward Velocity

When TCs move at a relatively fast forward velocity, the rain shield becomes displaced ahead of the circulation center (Corbosiero and Molinari 2003). The results of this study confirm this relationship between the forward displacement of rain shield and storm forward velocity. Isabel (Figure 3) has the fastest forward velocity of the 13 TCs in this study (9 m/s), and its outermost region (R8) was 27-30% occupied by the rain shield, while slower-moving TCs exhibited than 1% rain shield coverage in R8. Dennis (Figure 4) and Georges (Figure 2) are two examples of where a change in speed coincides with a change in the extent of the rain shield in the outer region of the storm. Dennis moved more quickly at landfall (2.9 m/s), and its R8 (R7) region was 3-5% (8-12%) full as compared to the period 24-40 hours post-landfall, when forward velocity slowed to 1.4 m/s and rain shield coverage decreased to less than 2% in R7 and R8. Georges moved at a speed of 1 m/s (3.7 m/s) during landfall (12-32 hours post-landfall) and at this time, rain shield coverage in R8 was less than 1% (10-13%).

3.3 Mountainous Terrain

When TCs encounter steeply elevated terrain, their precipitation amounts temporarily increase due to the enhanced uplift of moist air (Bender et al. 1985, Geerts et al. 2000). If the storm tracks on a perpendicular path towards the axis of the elevated terrain, precipitation is enhanced on the right side of the storm. Examples of this effect can be seen when Bret (Figures 5 and 6) approaches the Edwards Plateau in central Texas. The total areal coverage of the rain shield increases from 45000 to 90000 sq. km over a nine-hour period. The largest increase in areal coverage of the rain shield during this period occurs within the right rear quadrant.

3.4 Interaction with Middle Latitude Weather Systems

According to Hart and Evans (2001), 46% of Atlantic Basin TCs have transitioned into extratropical storms since 1950. During this process, an area of increased precipitation develops near the steep thermal gradient between the tropical and continental air masses typically located north of the storm's center (Klein et al. 2000). Two TCs analyzed in the current study transition into extratropical storms. When Isabel (Figure 7) and Gordon (Figure 8) become extratropical, the spatial extent of the rain shield increases on the left side of the storm in the outer regions, while decreasing on the right side and near the circulation center.

Interaction with frontal systems can also enlarge a TC's rain shield (Ulbrich and Miller 2001). After Helene (Figure 9) makes landfall over the Florida Panhandle, it encounters a frontal boundary located over northern South Carolina and Georgia. As Helene moves closer to this boundary, rainfall shifts to its two forward quadrants and the spatial extent of the rain shield increases. In fact, the rain shield at 28 hours post-landfall is larger than that at landfall, doubling in size to 120000 sq. km over that 28 hour period.

3.5 Strong Wind Shear

Strong directional wind shear prevents moisture from encircling the TC's center, thereby causing the rain shield to be asymmetrically distributed about the storm (Corbosiero and Molinari 2002). Five TCs in this study experience strong wind shear (Table 1). These storms have much smaller rain shields than storms that were not affected by strong wind shear. For example, Charley experiences strong southerly wind shear that confines its precipitation to the northern (right) side of its circulation (Figure 10).

4. CONCLUSIONS AND FUTURE RESEARCH

This paper describes how a GIS is used to spatially analyze the rain shields of 13 U.S. landfalling TCs. After the base reflectivity radar returns are converted into polygon shapes, a circular grid divides the rain shield into sections and the areal coverage of the rain shield within each section is calculated. Graphing this data over time shows that a) the rain shield of a hurricane (tropical storm or depression) covers (partially covers) the inner region of the storm; b) faster forward velocity coincides with a rain shield shift outwards from and ahead of the circulation center; c) movement near mountainous terrain increases the areal extent of the rain shield on the right side of the storm

track; d) an extratropical transition results in the rain shield's displacement to the left of the track and interaction with a frontal boundary can increase the areal extent of the rain shield; and e) strong wind shear can decrease the areal coverage of the rain shield and cause it to be asymmetrically-shaped.

Future research aiming to spatially analyze TC rainfall patterns within a GIS will be aided by the recent availability of radar data in GIS-compatible file formats (Ansari and Del Greco 2005). The analysis of additional TCs will allow a more precise quantification of rain shield changes over a longer period of record. Other techniques, including shape analysis (Wentz 2000), will also be employed to quantify the rain shield shapes themselves.

5. REFERENCES

Ansari, S. and S. Del Greco, 2005: GIS tools for visualization and analysis of NEXRAD radar (WSR-88D) archived data at the National Climatic Data Center. *21st International Conference on Interactive Information Processing Systems (IIPS) for Meteorology, Oceanography, and Hydrology*, San Diego, CA, AMS,

Bender, M. A., R. E. Tuleya and Y. Kurihara, 1985: A numerical study of the effect of a mountain range on a landfalling tropical cyclone. *Monthly Weather Review*, **113**, 567-82.

Cerveny, R. S. and L. E. Newman, 2000: Climatological relationships between tropical cyclones and rainfall. *Monthly Weather Review*, **128**, 9, 3329-36.

Corbosiero, K. L. and J. Molinari, 2002: The effects of vertical wind shear on the distribution of convection in tropical cyclones. *Monthly Weather Review*, **130**, 8, 2110-23.

Corbosiero, K. L. and J. Molinari, 2003: The relationship between storm motion, vertical wind shear, and convective asymmetries in tropical cyclones. *Journal of the Atmospheric Sciences*, **60**, 2, 366-76.

Geerts, B., G. M. Heymsfield, L. Tian, J. B. Halverson, A. Guillory and M. I. Mejia, 2000: Hurricane Georges's landfall in the Dominican Republic: Detailed airborne Doppler radar imagery. *Bulletin of the American Meteorological Society*, **81**, 5, 999-1018.

Harasti, P. R., C. J. McAdie, P. P. Dodge, W.-C. Lee, J. Tuttle, S. T. Murillo and F. D. Marks, 2004: Real-time implementation of single-doppler radar analysis methods for tropical cyclones: Algorithm improvements and use with WSR-88D display data. *Weather and Forecasting*, **19**, 2, 219-39.

Hart, R. E. and J. L. Evans, 2001: A climatology of the extratropical transition of Atlantic tropical cyclones. *Journal of Climate*, **14**, 4, 546-64.

Klein, P. M., P. A. Harr and R. L. Elsberry, 2000: Extratropical transition of western North Pacific tropical cyclones: An overview and conceptual model of the transformation stage. *Weather and Forecasting*, **15**, 4, 373-95.

Matyas, C. J., 2005: Using geographical information systems for the spatial analysis of base reflectivity radar data and applications to the study of tropical cyclone precipitation patterns. *15th Conference on Applied Climatology, American Meteorological Society*, Savannah, GA, American Meteorological Society,

Rao, G. V. and P. D. Macarthur, 1994: The SSM/I Estimated Rainfall Amounts of Tropical Cyclones and Their Potential in Predicting the Cyclone Intensity Changes. *Monthly Weather Review*, **122**, 7, 1568-74.

Rodgers, E. B., J. J. Baik and H. F. Pierce, 1994a: The environmental influence on tropical cyclone precipitation. *Journal of Applied Meteorology*, **33**, 5, 573-93.

Rodgers, E. B., S. W. Chang and H. F. Pierce, 1994b: A satellite observational and numerical study of precipitation characteristics in western North-Atlantic tropical cyclones. *Journal of Applied Meteorology*, **33**, 2, 129-39.

Ulbrich, C. W. and N. E. Miller, 2001: Experimental test of the effects of Z-R law variations on comparison of WSR-88D rainfall amounts with surface rain gauge and disdrometer data. *Weather and Forecasting*, **16**, 3, 369-74.

Wentz, E., 2000: A shape definition for geographic applications based on edge, elongation, and perforation. *Geographic Analysis*, **32**, 2, 95-112.

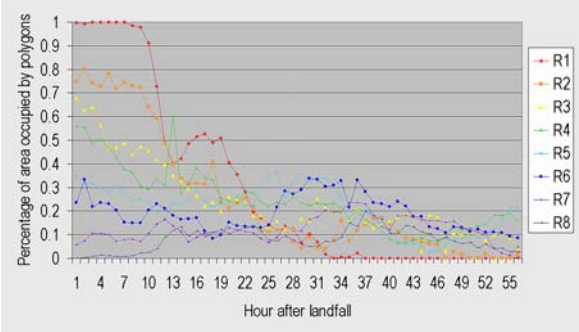

Figure 2. Coverage of rain shield within each annular ring for Georges (1998).

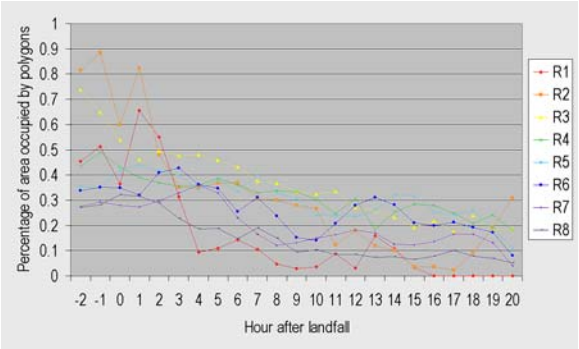

Figure 3. Coverage of rain shield within each annular ring for Isabel (2003).

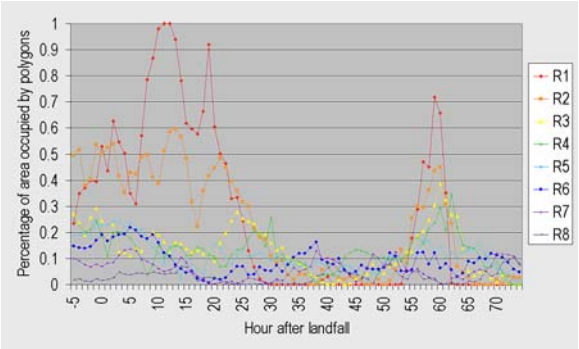

Figure 4. Coverage of rain shield within each annular ring for Dennis (1999).

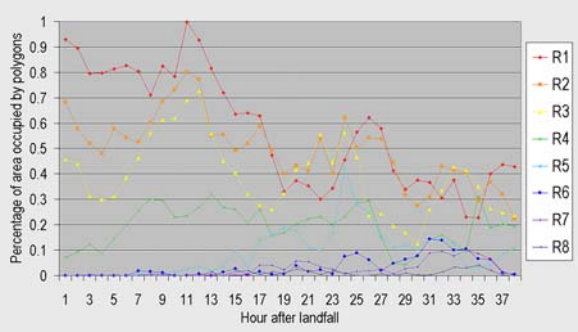

Figure 5. Coverage of rain shield within each annular ring for Bret (1999).

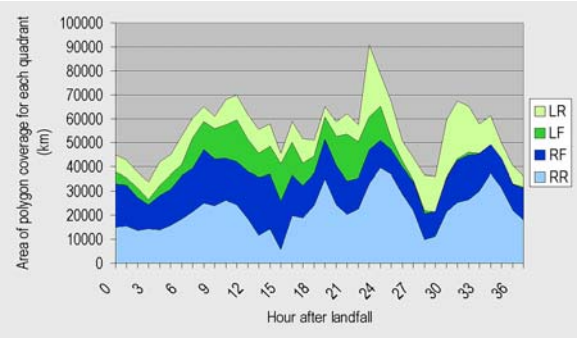

Figure 6. Total area covered by rain shield within each quadrant for Bret (1999).

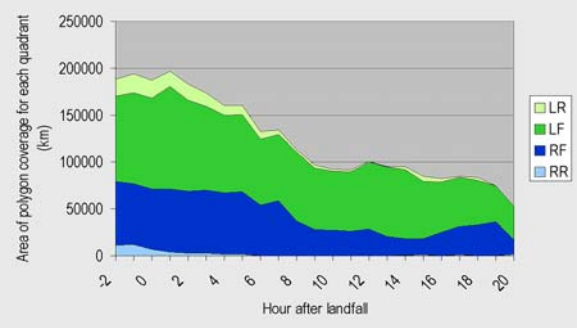

Figure 7. Total area covered by rain shield within each quadrant for Isabel (2003).

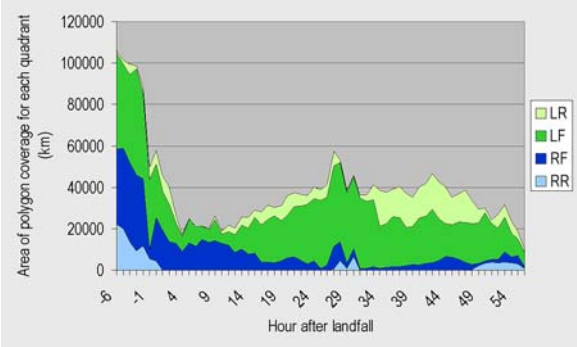

Figure 8. Total area covered by rain shield within each quadrant for Gordon (2000).

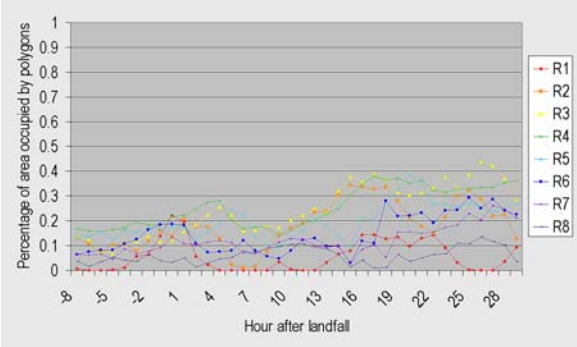

Figure 9. Coverage of rain shield within each annular ring for Helene (2000).

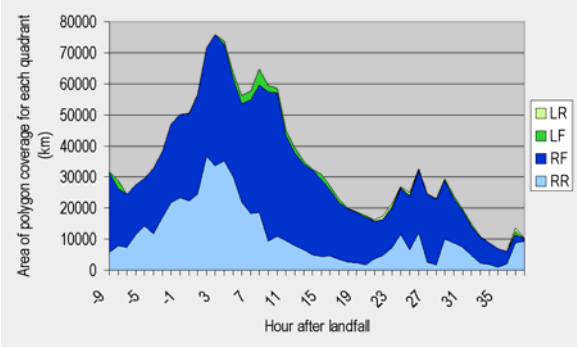

Figure 10. Total area covered by rain shield within each quadrant for Charley (1998).